IEEE Access
Multidisciplinary | Rapid Review | Open Access Journal

Received 29 March 2024, accepted 9 April 2024, date of publication 15 April 2024, date of current version 22 April 2024.

Digital Object Identifier 10.1109/ACCESS.2024.3388720

RESEARCH ARTICLE

Ambient Backscatter Communication System Empowered by Matching Game and Machine Learning for Enabling Massive IoT Over 6G HetNets

AMANY A. KHALIFA[1], AHMED M. ABD EL-HALEEM[2], (Member, IEEE), MAHMOUD M. ELMESALAWY[2], (Member, IEEE), AND HESHAM M. Z. BADR[2]

[1]Electronics and Communication Engineering Department, Egyptian Russian University, Cairo 11829, Egypt
[2]Electronics and Communication Engineering Department, Faculty of Engineering, Helwan University, Cairo 11795, Egypt

Corresponding author: Amany A. Khalifa (amany-ahmed@eru.edu.eg)

ABSTRACT Ambient backscatter communication (ABC) is considered as a promising paradigm for meeting the 6G massive Internet of Things (IoT) requirements which is expected to revolutionize our world. In this paper, a new multimode matching game and machine learning-based IoT ambient backscatter communication scheme is proposed to maximize the ABC system rate and capacity over the LTE and Wi-Fi multi-RAT heterogeneous network, thereby supporting the 6G green massive IoT communication. The proposed algorithm is designed to support different rate and capacity requirements for different massive Machine Type Communication (mMTC) use cases such as sensor networks, smart grid, agriculture and low data rate Ultra Reliable Low Latency Communication (URLLC) use cases such as tactile interaction. The proposed optimization algorithm runs into two phases, the first one is a matching game-based algorithm that selects the optimum association between the IoT tags and the primary users (PU) downlink signals from a specific base station which maximizes the IoT tags rate while minimizing the resulting interference to the PU. Each IoT tag can ride the PU downlink signal using one of three different riding modes according to the required IoT ABC system rate and capacity, whereas mode 1 allows multiple IoT tags to ride the whole PU downlink signal resource blocks, in mode 2 each IoT tag can ride only one subcarrier from the PU downlink signal resource blocks, while in mode 3 multiple IoT tags can ride the same subcarrier from the PU downlink signal resource blocks. In addition, unmanned aerial vehicles (UAVs) flying HetNodes equipped with LTE and Wi-Fi receivers are used as backscatter receivers to receive the IoT tags uplink backscattered signals, so the second optimization phase is formulated to maximize the total sum rate of the ABC system by dividing its service area into clusters using the enhanced unsupervised k-means algorithm, also the enhanced k-means algorithm finds the optimum location of each cluster's serving UAV flying HetNode that maximizes the channels gain between the IoT tags and the serving UAV flying HetNode in order to maximize the total system rate. The system model was implemented within the MATLAB environment where simulations across the various scenarios are conducted to assess the effectiveness of the proposed algorithm. Simulation results and the performance analysis demonstrated that the proposed algorithm can support the required rate for the most mMTC and low data rate URLLC IoT applications with average IoT tag rates in the range of 15 Kbps to 115 Kbps, and outperforms the algorithm-free riding technique in the case of massive IoT applications. The proposed mode 2 (first enhanced mode) achieves the best performance in terms of the average IoT tags rate and the total system rate with the lowest interference to the primary system users, on the other

The associate editor coordinating the review of this manuscript and approving it for publication was Zesong Fei.

© 2024 The Authors. This work is licensed under a Creative Commons Attribution-NonCommercial-NoDerivatives 4.0 License.
For more information, see https://creativecommons.org/licenses/by-nc-nd/4.0/

hand, mode 3 (second enhanced mode) improves the system capacity with maximum IoT tags satisfaction ratio. The capacity and satisfaction ratio of the proposed mode 3 outperforms mode 1 by 300% and 138% respectively and outperforms mode 2 by 2,000% and 420% respectively. The proposed algorithm reduces the interference power to the PUs on the average by $1 : (15.69 \times 10^{-12})$ relative to the algorithm-free riding technique. From the result, we can conclude that the proposed algorithm supports different IoT applications and achieves the required data rates with minimal effect on the primary system keeping the PU's data rate within the required range compared to the algorithm-free riding technique with the cost of higher time complexity.

INDEX TERMS IoT, ambient backscatter communication, 6G, LTE, Wi-Fi, multi-RAT, HetNets, HetNods, matching game, unsupervised machine learning, k-means, UAV.

I. INTRODUCTION

Internet of Things (IoT) is recognized as a dominant application for 6G networks, facilitating communication among devices. The proliferation of IoT devices has been substantial, demanding significant spectrum resources and energy which has become more challenging for the massive IoT network. Also, the 6G green communication is pivotal for energy efficiency, environmental sustainability, and cost reduction, it extends battery life for IoT devices, conserves resources, and upholds global responsibility for eco-friendly wireless networks. Ambient backscatter communication (ABC) is considered as a cutting-edge that receives the researcher's attention [1], [2], [3], [4], [5], [6], [7], [8], considered as one type of the passive backscatter communication (BC) which is an exceptionally promising solution for supplying power to a massive of IoT devices, solving the problem of longer communication range and supporting the green communication, improving system data rate, energy efficiency particularly those do not necessitate high data rates. Ambient backscatter technology represents a significant step towards sustainable wireless communication. By harvesting energy from the surroundings and transmitting data using minimal power, it aligns perfectly with the principles of green communication. This approach reduces the need for frequent battery replacements, lowering the environmental impact associated with battery disposal and production. Furthermore, it extends the operational life of battery-powered devices, reducing electronic waste and conserving resources. ABC benefits both URLLC and mMTC by providing low-power, instantaneous data transfer while conserving energy. In mMTC, it accommodates large numbers of IoT devices with its passive operation and minimal energy requirements, addressing scalability and device connectivity efficiently [9]. For most mMTC applications, the typical uplink data rate falls within the range of 1-100 kb/s (kb/s), serving the needs of Massive IoT implementations such as smart grids and agricultural monitoring [10], [11], [12], [13], [14]. On the other hand, low data rate URLLC applications such as tactile interaction can leverage ABC's capabilities to achieve their data rate requirements. The specific data rate for low data rate URLLC applications varies depending on the unique demands of each use case but typically ranges around 100 kb/s over the network [11].

Traditional ABC system consists of a Radio Frequency (RF) source as an ambient source, primary users (PUs), and secondary users (SUs), where the RF source is the existing Cellular or Wi-Fi signals, ABC doesn't require a dedicated carrier emitter. where the PU are the conventional active radio transmitters found in everyday wireless communication networks like cell phones. These devices continuously emit RF signals for data transmission and reception. on the other hand, SUs are battery-free devices, like tags or sensors which do not actively transmit RF signals like PUs but transmit binary bits (0 or 1) by altering the impedance state of their antennas, switching between reflecting and non-reflecting states [1].

A. LITERATURE REVIEW

In this section, we discuss the studies that attempted to improve IoT-ABC network performance by maximizing the total system data rate, capacity, and the IoT tags average rate in different networks. However, LTE base stations and Wi-Fi access points RF signals are utilized in many researches as ambient sources exploited to send the backscatter data [15], [16], [17], [18], [19], [20], [21], the heterogeneity of the network insufficiently exploited in the IoT based ABC which expected to strongly support the system requirements due to the extended continuous coverage. A backscatter system consists of UAVs serving a number of ground users and pairs of backscatter tags are considered in [22] where each backscatter pair has a transmitter and dedicated receiver, the backscatter transmitter sends its data by reflecting the UAV signal to its transmitter, to maximize the average rate of the backscatter pairs the authors proposed a joint optimization problem of user scheduling, the UAV's trajectory, and the transmit power. Authors in [23] considered a number of IoT tags and primary users in symbiotic radio communication HetNet. The authors proposed two optimization problems to maximize the sum rate of the IoT tags, in the first phase, a many-to-one matching game is employed for selecting the network (LTE or Wi-Fi) for information transmission. In this scenario, smartphones function as relays, delivering decoded IoT tag information to the Macro Base Station (MBS) or Wireless Access Point (WAP), thereby maximizing the overall system rate. The second phase of the solution involves the

utilization of the symbiotic radio technique. This facilitates IoT tags in reflecting their information to smartphones by backscattering the downlink signal between the MBS and smartphones. Subsequently, this information is decoded at the smartphones.

Authors in [24] considered routing and link scheduling for two network tiers, one tier consists of passive IoT tags and proposes a heuristic technique called the algorithm transmission set generator (ALGO-TSG) that constructs sets of transmissions for active RF links and backscattering links. It aims to maximize the number of links and activates additional power links for backscattering. The transmission sets generated by ALGO-TSG are used by a mixed-integer linear program (MILP) to derive a final schedule to optimize the active time of the backscattering links that maximizes the network throughput.

Authors in [25] propose an ABC system using OFDM-based structure, investigating phase shift keying (PSK) and delay shift keying (DSK) modulation schemes to realize higher data rates relative to the conventional ABC. The author in [26] investigated a multi-channel RF-powered cognitive backscatter network with one SU which can actively transmit its data packets if the selected channel is idle, if the channel is busy, it can harvest energy or backscatter data. Markov decision process is proposed to describe the action determination process, problem-based Markov decision process MDP is formulated to obtain the optimal channel-mode pair for the SU that maximizes the achieved average throughput.

The authors in [27] investigated two access control strategies in multi-RF backscatter networks for throughput maximization, the offline distributed access control strategy (DCA-S) is proposed when the channel information is available and the online combinatorial multi-armed bandit access control strategy (CMAB-S) is proposed in the case when the channel information is assumed to be unknown due the dynamics of the primary and the backscatter systems. The device association, the average throughput, and the number of admissible devices are investigated, showing better performance in typical scenarios.

In [28] the authors introduced an LTE backscatter system (Lscatter) exploiting that the LTE signal is a continuous RF source which makes it a perfect source for ABC, the design is evaluated using a testbed of backscatter hardware and USRPs in multiple real-world scenarios, 13.63 Mbps is achieved which is 368 times higher than the Wi-Fi backscatter communication frameworks.

In many studies [2], [2], [29] the number of backscatter devices is relatively small and the interference resulting from the backscattered signals has minimal impact on the system's primary users (PUs). However, when the network accommodates a substantial quantity of backscatter devices, the interference levels can exert substantial effects on the PUs, presenting new challenges and issues. Few research papers have studied and attempted to address the issue of interference caused by backscatter devices to the PUs.

Authors in [30] proposed a cognitive backscatter system with multi backscatter devices with only one backscatter receiver and one PU, a non-convex optimization problem is formulated to find the optimum transmitted power and reflection coefficient (RC) that maximize the sum rate of the backscatter devices considering the interference caused by the backscatter devices to the PU and keeping the PU signal to noise ratio greater than a threshold value. Furthermore, these backscatter devices can interfere with each other.

In [31] the authors considered one PU and multiple backscatter devices each with a backscatter receiver in coverage of one RF source. An optimization problem to find the optimum RC value with minimum base station transmitted power that maximizes the backscatter devices sum rate is formulated while considering the interference from the backscatter system to the PU, the proper control of reflection coefficient RC caused reduction in the outage by 40 points in the case o 150 SUs.

B. CONTRIBUTION

This work proposes a novel matching game and machine learning-based multimode optimizing algorithm that optimizes the IoT-ABC system rate, capacity, and IoT tags satisfaction ratio taking into consideration the interference effect on the heterogenous 6G primary network which consists of LTE and Wi-Fi coverage. Implementing this approach exploits the OFDM structure efficiently by considering the transmission on subcarrier level, whereas the aforementioned works send the tags data over OFDM symbol level. Additionally, the proposed algorithm strongly supports different rate requirements for most mMTC and low data rate URLLC applications with minimum interference effect on the PUs. However, by adding the new dimension of deploying backscatter communication in HetNet, it will be more challenging to solve some problems such as finding the optimum association between IoT backscatter tags and the deployed RF sources, especially when considering the interference caused by the IoT tags to the PUs. Moreover, we considered the UAV as a flying HetNode carrying both Wi-Fi and LTE backscatter receivers to serve the IoT tags in a sub-area called cluster with a selected location to improve the overall system rate. Therefore, we formulated an optimization problem to find the optimum association between IoT tags and the RF sources and proposed an approach to provide the optimum UAV location that maximizes the IoT tag's sum-rate.

The contribution of this paper can be summarized as follows:

1) To the best of our knowledge, the proposed multimode optimization algorithm is the first one optimizing the performance of multiple ambient backscatter IoT tags as a backscatter transmitter, and flying UAV contains LTE and Wi-Fi backscatter receivers over a 6G Heterogenous Network consists of LTE macro and small cells and Wi-Fi access point coverage.
2) The proposed algorithm introduces three different riding modes, the first mode is the default where a number

of IoT tags can share the riding of the PU downlink RF OFDM signal resource blocks. The second mode or the first enhanced mode where each IoT tag rides one subcarrier from the PU downlink RF signal resource blocks. The third mode is a combination of the first and second ones (the second enhanced mode) where each group of IoT tags share the riding of one subcarrier of the PU downlink RF signal.

3) The proposed optimization problem is formulated to maximize the IoT tag's total system rate, system capacity, and IoT tags satisfaction ratio whereas the rate requirements for the PUs are satisfied. The problem is solved sequentially in two phases as two independent sub-problems.
4) In the first phase, an optimization problem is formed to find the optimum association between IoT tags and the PU downlink signals from a selected base station. The formulated problem is solved using a matching game algorithm considering a multi-RAT HetNet environment while minimizing the interference caused by the backscattered signals to the PUs.
5) An optimization problem is formulated in the second phase to find the optimum tags clustering and the UAV flying HetNode optimum location for each cluster which maximizes the overall system data rate.
6) An enhanced unsupervised machine learning k-means algorithm is used to cluster the IoT tags and find the optimum UAV flying HetNode location for each cluster.
7) The proposed modes can support different ABC IoT system requirements, where one can support most massive IoT applications (mMTC), another one can achieve the required tags rate for low data rate URLLC applications, and the last reduces the interference effect on the primary system users.
8) Simulation results showed the effectiveness of the proposed algorithm, which yields a significant performance enhancement compared to the algorithm-free riding technique that can be used on the same framework. Also, the results showed improvement in the IoT tags rate, total system rate, capacity, and satisfaction ratio with minimum interference on the primary system users.

The remainder of this paper is organized as follows. In section II, we proposed the system model and the data rate calculations. In section III, we proposed the two formulated optimization problems. In section IV we present the detailed matching game algorithm. In section V the proposed k-means++ algorithm is explained in detail. The performance of the proposed framework is evaluated in VI. Finally, we conclude the paper in section VII.

II. SYSTEM MODEL AND THE DATA RATE CALCULATIONS

A. SYSTEM MODEL

In this section, ambient backscatter communication system over downlink data transmission in 6G heterogenous communication network is considered. The proposed system consists of two subsystems as shown in Fig. 1 and can be demonstrated as follows:

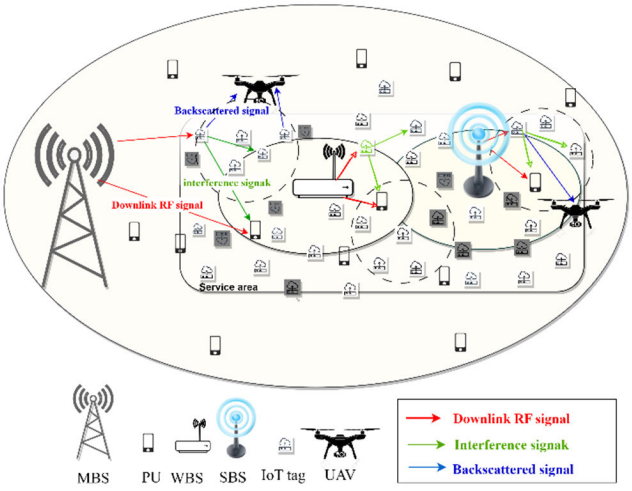

FIGURE 1. System model.

Primary System: A 6G multi-RAT heterogeneous network comprised of a Small Base Station (SBS), and Wi-Fi access point (WAP) under the coverage of a Macro Base Station (MBS), these three base stations are referred as RF sources in the rest of this paper and is assumed to serve N number of PUs represented by the set $\mathcal{N} = \{1, 2, \ldots, n, \ldots, N\}$ with cardinality N, getting into consideration that each PU had a specific rate requirement must be satisfied. On the other hand, the set of RF sources is denoted by $\mathcal{B} = \{1, 2, 3\}$, where $b = 1$ refers to the WAP, $b = 2$ refers to the SBS, and $b = 3$ represents the MBS.

Secondary System: The secondary system consists of K number of backscatter IoT tags as secondary users distributed in a service area and represented by set $\mathcal{K} = \{1, 2, \ldots, k, \ldots, K\}$ with cardinality K. The backscatter IoT tags in the service area are clustered using k-means algorithm to M number of clusters, each cluster is served by a UAV flying HetNode equipped with LTE and Wi-Fi ambient backscatter receivers. The number of M serving UAV flying HetNodes are represented by set $\mathcal{M} = \{1, 2, \ldots, m, \ldots, M\}$ with cardinality M.

In the proposed system model, the IoT tags first associate one base station to exploit the existence of the primary RF sources, then select a PU's downlink signal to ride using one of the riding modes, and send their data to the serving UAV flying HetNode. Each IoT tag sends its data by reflecting a fraction α of the PU's downlink RF signal, where $\alpha_j \in [0, 1]$ called the backscatter reflection coefficient of the source signal power.

The proposed multimode algorithm has three riding modes used to demonstrate how the IoT tags ride the base station downlink RF signal to efficiently use the OFDM signal structure, support rate, and capacity requirement for most mMTC and low data rate URLLC IoT applications, these three modes can be outlined as follows:

1. **The first mode (default mode):** In this mode, each IoT tag rides the resource blocks of the OFDM downlink signal dedicated for the selected primary user (PU). Additionally, multiple IoT tags can share the riding of the same resource blocks, provided that the resulting interference does not impact this PU's data rate requirements.
2. **The second mode (1st enhanced mode)**: in this mode, the IoT tag can reserve and utilize only one subcarrier from the allocated downlink OFDM resource blocks for the selected primary user (PU) [32], where each OFDM subcarrier is solely allocated for only one IoT tag. So, each PU downlink OFDM resource blocks can be utilized by a number of IoT tags equivalent to the number of subcarriers and there is no interference between all IoT tags share that PU downlink OFDM resource blocks.
3. **The third mode (2nd enhanced mode):** in mode 3 each IoT tag can ride one subcarrier of the selected PU's downlink OFDM resource blocks. Also, multiple IoT tags can share the riding of the same subcarrier as long as the resulting average interference doesn't affect this PU's data rate requirements.

B. IoT TAGS DATA RATE CALCULATIONS

As the service area is divided into M clusters (sub-areas), so there are M number of flying UAV HetNodes, each UAV flying HetNode $m \in \mathcal{M}$ provides a wireless coverage of radius R_m at a fixed altitude H_m, and its location in the free space can be represented as (x_m, y_m, z_m), where x_m, y_m, z_m are the UAV's x, y, and z 3-D location in the free space, $z_m = H_m$. Also, each IoT tag $k \in K$ location can be represented as (x_k, y_k, z_k). The path loss between UAV flying HetNodes and the IoT tag can be represented by considering the Line of Sight (LoS) and Non-Line of Sight (NLoS) probabilities as follows [33] and [34].

$$PL_{k,m} = p^{LOS}_{k,m} L^{LOS}_{k,m} + p^{NLOS}_{k,m} L^{NLOS}_{k,m} \tag{1}$$

where $p^{LOS}_{k,m}$ and $p^{NLOS}_{k,m}$ are the probabilities of LoS and NLoS between IoT tag k and its UAV receiver m respectively, such that $p^{LOS}_{k,m} + p^{NLOS}_{k,m} = 1$, $L^{LOS}_{k,m}$ and $L^{NLOS}_{k,m}$ are the average LoS and NLoS path loss respectively which can be calculated as follows.

$$p^{LOS}_{k,m} = \frac{1}{1 + a\, exp(-\sigma\left[\theta_{k,m} - a\right])} \tag{2}$$

where a, σ are constant in the urban and rural environment called S-curve parameters, and $\theta_{k,m}$ is the elevation angle which equals

$$\theta_{k,m} = \frac{180}{\pi} \times sin^{-1}\left(\frac{H_m}{D_{k,m}}\right) \tag{3}$$

$$L^{LOS}_{k,m} = \mu_1 \left(\frac{4\pi f_c D_{k,m}}{c}\right)^{\delta} \tag{4}$$

$$L^{NLOS}_{k,m} = \mu_2 \left(\frac{4\pi f_c D_{k,m}}{c}\right)^{\delta} \tag{5}$$

where $D_{k,m}$ is the distance between the IoT tag k and its serving UAV flying HetNode m.

$$D_{k,m} = \sqrt{(x_k - x_m)^2 + (y_k - y_m)^2 + (z_k - z_m)^2} \tag{6}$$

μ_1 and μ_2 are the extreme path loss coefficients in LoS and NLoS, δ is the path loss exponent, f_c denotes the carrier frequency and c is the speed of light. Finally, the gain of the air-ground channel is calculated using (1) as $h_{k,m} = \frac{1}{PL_{k,m}}$ [33], [35].

Since each IoT tag rides the downlink signal of a PU to backscatter its data, the UAV flying HetNode receiver recovers the IoT tag signal using Successive Interference Canceler (SIC) by firstly decodes the signal for the PU, treating the backscattered signals as interference signals. It then subtracts the decoded PU signal from the received signal and proceeds to decode the signal from its corresponding transmitter.

The signal-to-interference noise ratio (SINR) for the IoT tag k receiver when rides the base station b downlink RF signal is:

$$\gamma^{b}_{k,m} = \frac{\alpha_k P^{b}_{t} g_{b,k} h_{k,m}}{I_k + \sigma^2} \tag{7}$$

where α_k is the backscatter reflection coefficient of the tag k, $h_{k,m}$ is the channel gain coefficient between IoT tag k and the UAV flying HetNode m, P^{b}_{t} denotes the downlink transmitted power from base station $b \in \mathcal{B}$ where $b = 1$ refers to the WAP, $b = 2$ refers to the SBS, and $b = 3$ represents the MBS, and $g_{b,k}$ is the channel gain between base station b and the IoT tag k. So, the term $\alpha_k P^{b}_{t} g_{b,k}$ represents the amount of reflected signal power (IoT tag information signal power $P^{IoT}_{k,b}$) from the IoT tag and transmitted to the serving UAV flying HetNode. Also, σ^2 denotes the additive noise power over each channel, and I_k expresses the interference between this IoT tag and the other tags ride the same PU signal in the same cluster m, where $I_k = \sum_{j,j\neq k} \alpha_j P^{b}_{t} g_{b,j} h_{j,m}$.

Finally, based on SINR in (7) the IoT tag k achieved data rate $R^{b}_{k,m}$ can be calculated using Shannon formula [23] as follows.

$$R^{b}_{k,m} = W_{k,m} log_2\left(1 + \gamma^{b}_{k,m}\right) \tag{8}$$

where $W_{k,m}$ is the channel bandwidth between the IoT tag and its serving UAV flying HetNode.

C. PRIMARY USER DATA RATE CALCULATIONS

For LTE PUs, radio channels for each base station are assumed to be allocated equally among the associated devices and the transmitted power of each base station is allocated equally among the available radio channels. thus, when PU n where $n \in N$ is associated with the base station $b \in \mathcal{B}$, the PU SINR can be calculated as follows:

$$\gamma_{b,n} = \frac{P^{b}_{t} g_{b,n}}{I_n + \sigma^2} \tag{9}$$

where P^{b}_{t} denotes the downlink transmit power from base station $b \in \mathcal{B}$, $g_{b,n}$ is the channel gain between the base

station b and the PU n, the term I_n represents the interference from the IoT tags ride the PU n downlink signal, where $I_n = \sum_i \alpha_k g_{b,k} P_t^b f_{k,n}$, $g_{b,k}$ is the channel gain between the interfering IoT tag k and the associated base station b, $f_{k,n}$ is the channel gain between the interfering IoT tag k and the PUn, α_k is the backscatter coefficient of IoT tag k [36], [37].

Based on the previous SINR calculation in (9), the rate $R_{b,n}$ of each PU $n \in N$ can be determined simply by Shannon model as follows:

$$R_{b,n} = W_{b,n} log_2 \left(1 + \gamma_{b,n}\right) \tag{10}$$

where $W_{b,n}$ is the bandwidth of the PU channel.

III. PROBLEM FORMULATION

In this paper, we focus on finding the optimum IoT tag association with RF sources (LTE and Wi-Fi base stations), grouping the IoT tags within the service area into clusters, each cluster served by one UAV flying HetNode as an ambient backscatter receiver, then finding the optimum UAV flying HetNode location on each cluster in order to maximize the total sum rate of the ambient backscatter system taking into account the PU's rate requirement, this optimization problem is considered as an NP-complete problem and can be formulated as follows:

$$\begin{aligned} &\max_{\Psi, x_u, y_u} \sum_{k\in\mathcal{K}} \sum_{b\in\mathcal{B}} \sum_{n\in\mathcal{N}} \sum_{m\in\mathcal{M}} \Psi_{k,b,n,m} R_{k,m}^b \\ &\text{Subject to,} \quad C1: \Psi_{k,b,n,m} = \{0, 1\} \\ &\qquad C2: \sum_{b\in\mathcal{B}} \sum_{j\in\mathcal{N}} \sum_{m\in\mathcal{M}} \Psi_{k,b,n,m} = 1 \quad \forall k \in K \\ &\qquad C3: 0 \le \alpha_k \le 1 \forall k \in K \\ &\qquad C4: R_{b,n} \ge R_n^{th} \quad \forall n \in N, b \in \mathcal{B} \\ &\qquad C5: z_m = H_m \end{aligned} \tag{11}$$

where constraint C1 indicates that the association matrix $\Psi_{k,b,n,m}$ is a binary variable, denotes that the IoT tag k associated with the base station b, rides the downlink signal of primary user n and forwards its data to the UAV flying HetNet m, such that 0 denotes that IoT tag k is not associated, while 1 denotes that IoT tag is associated. Constraint C2 implies that an IoT tag k can only and must be associated with one base station at a time riding one PU signal and belonging to one cluster. In addition, constraint C3 ensures that the IoT tag's backscatter reflection coefficient will be between 0 and 1. Constraint C4 is used to limit the effect of the backscatter system on the primary system by ensuring that the PU's data rate will be within acceptable levels above a given threshold R_n^{th}. To solve This NP optimization problem tractably, it will be divided into two independent sub-problems and solved through two phases as follows.

The first sub-problem (12), solved using a stable matching game algorithm to maximize the IoT tag k received signal strength $P_{k,b,n}^r$ when associated with the base station b, in order to maximize the overall system rate by finding the optimum association between IoT tags and the RF sources (LTE or Wi-Fi) and selecting a PU's RF downlink signal to ride while keeping the resulting interference level caused by these IoT tags to that PU within the acceptable limits to ensure that the rate requirements are assured, the expected service is delivered and the PU data rate is greater than a predefined threshold R_n^{th} for all $n \in N$ at all times. This can be formulated as follows.

OPT1: IoT tags association

$$\begin{aligned} &\max_{\Psi} \sum_{k\in\mathcal{K}} \sum_{b\in\mathcal{B}} \sum_{n\in\mathcal{N}} \Psi_{k,b,n} P_{k,b,n}^r \\ &\text{Subject to,} \quad C1: \Psi_{k,b,n} = \{0, 1\} \\ &\qquad C2: \sum_{b\in\mathcal{B}} \sum_{j\in\mathcal{N}} \Psi_{k,b,n} = 1 \forall k \in K \\ &\qquad C3: 0 \le \alpha_k \le 1 \quad \forall k \in K \\ &\qquad C4: R_{b,n} \ge R_n^{th} \quad \forall n \in N, b \in \mathcal{B} \end{aligned} \tag{12}$$

where each IoT tag sends an association request to the base station that has the best received signal strength to provide the most amount of received power to that IoT tag, this will achieve higher tags data rates.

The second sub-problem (13) aims to cluster the service area to M clusters and find the optimum location of the UAV flying HetNode for each cluster that maximizes the IoT tags signal-to-interference and noise ratio in order to maximize the overall backscatter system rate. The enhanced unsupervised machine learning K-means algorithm is proposed to solve this problem by dividing the IoT tags in the service area into a number of clusters each cluster served by a UAV flying HetNode, with serving location point ensuring maximum channel gain between IoT tags and their serving UAV flying HetNode backscatter receiver.

K-means++ algorithm aims to group the IoT tags into M clusters and computes the centroid of each cluster while effectively minimizing the distance from the IoT tags and their cluster centroid and maximizing the separation between clusters' centroids. The centroid for each cluster is considered to be the optimum UAV flying HetNode location for this cluster. This strategic deployment reduces the distances $D_{k,m}$ between the IoT tags and their corresponding serving UAVs, thus minimizing the UAV channel path losses $L_{k,m}^{LOS}$ and $L_{k,m}^{NLOS}$ in (4) and (5) respectively. Additionally, interference among IoT tags in different clusters is minimized due to the maximal separation between cluster centroids and can be neglected. Consequently, the SINR $\gamma_{k,m}^b$ in (7) and the rate in (8) are maximized for the IoT tags. Based on this, the second optimization problem can be formulated as follows.

OPT2: UAV flying HetNodes locations.

$$\begin{aligned} &\max_{x_u, y_u} \sum_{k\in\mathcal{K}} \sum_{b\in\mathcal{B}} \sum_{n\in\mathcal{N}} \sum_{m\in\mathcal{M}} \Psi_{k,b,n,m} R_{k,m}^b \\ &\text{Subject to,} \quad C1: \Psi_{k,b,n,m} = \{0, 1\} \\ &\qquad C2: \sum_{b\in\mathcal{B}} \sum_{j\in\mathcal{N}} \sum_{m\in\mathcal{M}} \Psi_{k,b,n,m} = 1 \quad \forall k \in K \end{aligned} \tag{13}$$

IV. MULTIMODE MATCHING GAME-BASED BACKSCATTER IoT TAGS ASSOCIATION

The matching game is a mathematical algorithm used to solve optimization problems with improved performance and low complexity. In this paper, a two-sided many-to-one matching game algorithm is used to solve the first formulated optimization problem by finding the optimal backscatter IoT tags association while ensuring delivering the required rate of PUs under the effect of associated IoT tags interferences.

In the proposed technique the LTE and Wi-Fi base stations and their primary users are one side of the game and the backscatter IoT tags are the other side, where each IoT tag sends an association request to the primary system to ride the downlink PU signal depending on the IoT tags' preference list which determined using their utility functions considering the interfering power to the PU and the received power from the base stations which serving this PU, each PU accepts or rejects this request according to its preference determined using the utility function and its quota.

A. MATCHING GAME ALGORITHM DEFINITION

The association problem can be formulated as many-to-one matching game with a tuple $(\mathcal{N}, \mathcal{K}, \succ_n, \succ_k)$. In which $\succ_{\mathcal{N}} = \{\succ_n\}_{n\in\mathcal{N}}$ and $\succ_{\mathcal{K}} = \{\succ_k\}_{k\in\mathcal{K}}$ denotes the preference relations of the PUs and the IoT Tags respectively. The matching game is defined by μ_{TA}:$\mathcal{K}\rightarrow\mathcal{N}$, where μ_{TA} is the tags association outcome of the matching game. Let $U_k(n)$ and $U_n(k)$ denote IoT tag k and PU n utility functions respectively in which they are used to construct preference relations for choosing the best match. The PU quota is calculated based on the riding mode as the maximum number of IoT tags that can ride the PU downlink signal with an acceptable effect on the PU's data rate $R_n \geq R_n^{th}$ for mode 1 and mode 3. In mode 2 the PU's quota equals the number of allocated subcarriers, where each IoT tag will be matched to at most only one PU subcarrier i.e. each PU can accept a maximum number of IoT tags equal to its resource blocks (RB) times the number of subcarriers per resource block.

B. IoT TAGS UTILITY FUNCTION

In the context of the first formulated optimization problem, the IoT tag's utility function considers two important parameters, the interfering power to the PU and the tag received power from the RF base station with which the PU is already associated. This utility function can be expressed as follows:

$$U_k(n) = P^r_{k,b} + I^{-1}_{k,n} \tag{14}$$

where $U_k(n)$ represents the IoT tag k utility function when it rides the PU n signal, $I^{-1}_{k,n}$ is the normalized interfering power caused by the IoT tag k to the PU n and $P^r_{k,b}$ is the IoT tag k normalized received power from the RF base station b which the PU n associated with, it can be calculated as follows.

$$P^r_{k,b} = \frac{P^b_t}{PL_{k,b}} / P^r_{max} \tag{15}$$

where P^b_t is the transmitted power from the RF base station b (LTE or Wi-Fi), $PL_{k,b}$ is the free space path loss between IoT tag k and the RF source b and P^r_{max} is the maximum received power of IoT tags. The interfering power to the PU n associated with the base station $bI^{-1}_{k,n}$ caused by the IoT tag k when rides the signal of this PU can be calculated by the following formulas.

$$I_{k,n} = \alpha_k g_{b,k} P^b_t f_{k,n} \tag{16}$$

C. PRIMARY USER UTILITY FUNCTION

The primary user's utility function must be efficiently designed in such IoT tags association problem. Each PU accepts the IoT tags riding request as the interference caused by the IoT tags has a minimum effect on the PU's data rate.

based on the PUs rate requirements, its utility can be represented by:

$$U_n(k) = R_{b,n}(k) \tag{17}$$

where $R_{b,n}$(k) is the PU n achieved data rate if IoT tag k rides its downlink RF signal from base station b.

D. MULTIMODE MATCHING GAME ALGORITHM FOR IoT TAGS ASSOCIATION

The details of the proposed multimode matching game-based IoT tags association algorithm are described in Algorithm 1. After initialization, each IoT tag constructs its preference list $\succ_k$ using (14) and sends a biding request $b_{k\rightarrow n} = 1$ to PU n with the highest utility (lines 4-5). In order to find a stable matching $\mu_{TA}(k)$ for the IoT tags, each PU inserts all requesting tags into the set I^{req}_n and construct its preference relations for I^{req}_n based on (17) (lines 7-8).

Based on the selected mode from the multimodes, PUs accept biding IoT tags and update their matched list I_n under the matching $\mu_{TA}(k)$ until reaching its maximum allowable number of devices according to its quota, and rejects the rest of the biding IoT tags such that $I^{rej}_n = \{I^{req}_n \backslash I_n\}$(lines 10-13). Each IoT tag in the rejected list I^{rej}_n removes PU n from its preference relation $\succ_k$ (line 14). The process is repeated with a maximum of N times until there are no biding IoT tags.

Considering the change in network conditions the algorithm should be executed every T time period to avoid frequent association switching that may cause Ping-Pong effects. To obtain stable matching in the proposed matching game algorithm, let us denote the subset of all possible matchings between $\mathcal{N}$ and $\mathcal{K}$ by $\mu_{TA}(k, n)$. A pair $(k, n) \neq \mu_{TA}$, where $n \in \mathcal{N}, k \in \mathcal{K}$ is said to be a blocking pair for the matching μ_{TA} if it is not blocked by an individual tag k and PU n, and there exists another matching $\mu_{TA}{}' \in \mu_{TA}(k, n)$ such that IoT tag k and PU n can achieve a higher utility. Hence, given fixed preference relations of IoT tags and PUs, Algorithm 1 is known as the deferred acceptance algorithm in the two-sided matching which converges to a stable matching [38], [39].

The multimode-based association between IoT tags and the N number of PUs served by the LTE and Wi-Fi RF sources is assumed to be in one of three modes as follows:

Algorithm 1 Matching Game for IoT Tags Association

- Input: Initialize, N, K, B.
- Discovery and utility functions calculations:

1: Every IoT tag k construct $\succ_k$ using $U_k(n)$
- Finding a stable Matching:

2: While $\sum_{\forall_{k,n}} \boldsymbol{b}_{k\to n} \neq \mathbf{0}$ do:
3: For each unassociated tag:
4: Find $n = \arg \max_{\mathrm{n} \in \succ_k} U_k(n)$.
5: Send a request $b_{\mathrm{k}\to\mathrm{n}} = 1$ to PU n.
6: For all PU n:
7: Update $\mathrm{I}_n^{req} \leftarrow \{k{:}b_{\mathrm{k}\to\mathrm{n}} = 1, k \in \mathcal{K}\}$.
8: Construct $\succ_n$ based on U_n(k).
9: repeat
10: Accept $k = arg \max_{k \in \succ_n} U_n(k)$.
11: Update $\mathrm{I}_n \leftarrow I_n \cup k$
12: until ($R_{b,\mathrm{n}} \geq R_{th}^n$ for mode1 and 3, $\mathrm{I}_n \leq 12{*}\mathrm{RB}$ for mode 2).
13: Update $I_n^{rej} \leftarrow \left\{I_n^{rej}/\mathrm{I}_n\right\}$.
14: Remove PU $n \in \succ_k, \forall_k \in I_n^{rej}$
15: end while
16: Outputs: A stable matching μ_{TA}^*

- **Mode 1 (default association mode):** in this mode, the IoT tags associate a base station and ride the resource block allocated to a specific PU served by this base station. In this case, the IoT tag association request is accepted as long as the total resulting interference to that PU is kept within a predefined threshold where the PU data rate is greater than R_n^{th}, each tag exclusively utilizes the entire 180 kHz signal of the PU.
- **Mode 2 (1st enhanced mode):** in this mode, each IoT tag can associate a base station and ride one subcarrier of the resource block allocated to a specific PU served by that base station so each PU can accept 12 IoT tags per resource block and there are no interfering signals between the associated IoT tags.
- **Mode 3 (2nd enhanced mode):** this mode is a combination of the previous two modes where a group of IoT tags can associate a base station serving a PU and ride one subcarrier of this PU signal, each tag can utilize the one subcarrier 15 kHz bandwidth signal as long as the resulting average interference caused by the tags is kept within a predefined threshold where the PU data rate is greater than the R_n^{th}.

V. ENHANCED K-MEANS ALGORITHM-BASED BACKSCATTER IoT TAGS CLUSTERING

To solve the second formulated optimization problem of clustering the IoT tags within the service area into a number of clusters and finding the optimum UAV flying HetNodes locations that maximize the system rate, an unsupervised machine learning (ML) k-means algorithm is proposed to group the K number of tags into M number of clusters then consider the centroid of each cluster as the optimum location of the cluster UAV HetNode backscatter receiver.

The k-means algorithm for user clustering is studied in [40] and can be defined as an iterative data-partitioning algorithm and one of the most commonly used unsupervised machine learning algorithms to partition users in the communication area into separate clusters. One disadvantage of the k-means algorithm is that it is very sensitive to the centroid initializations [41]. Also, if the initial centroid is a far point it might not be associated with any other points. Equivalently, more than one initial centroid might be created into the same cluster which leads to poor grouping. In this section, k-means++ algorithm is developed to solve this issue. It aims to provide a clever initialization of the centroids that improves the quality of the grouping process and the running time of the k-means algorithm [42]. The details of the proposed algorithm are described in algorithm 2, in line 2 an initial centroid c_1 is selected randomly and the euclidean distances from each tag k to this centroid are calculated as follows $d(x_k, c_j) = \|x_k - c_j\|$ where x_k is the tag location then selects the next centroid (lines 3-4), the remaining centroids are selected with probability p_k as in line 5 based on the maximum squared distance to make the centroid as far from the other centroids as possible and the process is repeated until all K centroid seeds are chosen.

After repeating line 5 M times as considered in line 6, the initial centroids of the M clusters are chosen based on maximizing the distances between centroids which minimizes the possibility of interference between clusters. The Euclidean distance for each tag and the cluster centroid are calculated and each tag is assigned to the closest centroid, so each tag belongs to the group served by the closest M^{th} UAV flying HetNode for improving the grouping of completed forms according to the channel conditions between the serving UAV flying HetNode and the IoT tags groups. Repeat the group formation for all tags until convergence (lines 7-9).

The result of this algorithm is the optimal IoT tags clusters with minimum distance between IoT tags and their serving UAV flying HetNode, which maximizes the channel gains between them and positively affects the total system rate. The clever initialization of the centroids using k-means++ maximizes the distances between the UAV flying HetNodes, which minimizes the interference between the UAV flying backscatter receivers and enhances the system rate.

VI. PERFORMANCE EVALUATION

In order to show the effectiveness of the proposed framework the performance of the system is evaluated using the MATLAB software by randomly deploying backscatter IoT tags within a service area covered by 6G multi-RAT HetNet consisting of SBS and WAP under the coverage of MBS and comparing our proposed algorithm with algorithm-free riding technique where the association of the IoT tags with the PUs and the ambient RF sources done in random manner, after that the associated IoT tags clustered into M clusters using k-means++ algorithm.

Algorithm 2 proposed IoT Tags Clustering Scheme

1. **Input:** K, M, locations of IoT tags
2. **Select** an IoT tag uniformly at random from the distributed IoT tags in the service area. The chosen IoT tag location is the first centroid and is denoted c_1.
3. **Compute** the distances from each tag to c_1. Denote the distance between c_j and the observation h as d (x_h, c_j).
4. **Select** the next centroid, c_2 at random with probability $\frac{d^2(x_k,c_1)}{\sum_{j=1}^{k} d^2(x_j,c_1)}$
5. To choose center j:
   Compute the distances from each tag to each centroid, and assign each tag to its closest centroid.
   For $k = 1, \ldots,$ K and $p = 1, \ldots, j-1$, select centroid j at random from X with probability $p_k = \frac{d^2(x_k,c_p)}{\sum_{\{a:x_a \epsilon C_p\}} d^2(x_a,c_p)}$ where C_p is the set of all tags closest to the centroid c_p and x_h belongs to c_p.
6. **Repeat step 5** until M initial centroids seeds are chosen.
7. **Compute** tag to cluster centroid Euclidean distances from all tags to each centroid
8. **Compute** the average of the tags in each cluster to obtain M new centroid locations.
9. Repeat steps 7 and 8 until cluster assignments do not change.
10. **Output:** Optimal IoT tags clusters with minimum distance between IoT tags and their centroids.

A. SIMULATION SETUP

Consider a service area of size 300 m × 100 m with a uniform distributed K backscatter IoT tags deployment, the service area served by M number of UAV flying HetNodes, and there are N number of PUs under the coverage of the MBS.

The path loss model for the MBS users can be calculated as

$$PL^m = 128.1 + 37.6 \times log_{10}(D_m) \quad (18)$$

where D_m is the distance in km between MBS and the system users.

On the other hand, the path loss model for the SBS can be approximated by the following equation.

$$PL^s = 140.7 + 36.7 log_{10}(D_s) \quad (19)$$

where D_s is the distance in km between the SBS and the system users [38], [43].

For the Wi-Fi coverage area, the indoor Wi-Fi path loss model is considered and represented as follows

$$PL^W = 20 log_{10} f_w + \eta_w log_{10} D_w + P_f(n_{walls}) - 28 \quad (20)$$

Such that D_w is the distance in meters between system users and WAP, f_w is the Wi-Fi transmission frequency in MHZ, η_w is the distance power loss coefficient and is assumed to be 30, n_{walls} is the number of walls which is assumed to be 3 and $P_f(n_{walls}) = 13 + n_{walls}$ is the penetration loss factor [38].

TABLE 1. Simulation parameters.

LTE Parameters	
Transmit power of MBS	46 dBm
MBS radius	1000m
Transmit power of SBS	20 dBm
Channel bandwidth	20 M Hz
Number of subcarriers per resource block.	12
Subcarrier spacing	15 K Hz
Noise power	-174 dBm/Hz
Wi-Fi parameters	
Wi-Fi bandwidth	20 M Hz
Transmit power of WAP	200 mw
Wi-Fi technology	IEEE 802.11n
Wi-Fi carrier frequency	2.4 GHz
Secondary system simulation parameters	
UAV altitude.	30m
Number of serving UAV flying HetNodes (Number of clusters).	5
Number of resource blocks allocated for each PU.	1
Allocated LTE channel bandwidth for each PU	180 K Hz
IoT tag modulation technique [20],[44].	QPSK

To model the channel gains between the PUs and the IoT tags, the path loss can be calculated as follows.

$$PL^{k,n} = 30.6 + 36.7 log_{10}(D_{k,n}) \quad (21)$$

where $D_{k,n}$ is the distance in meters between the PUn and the IoT tag k [45].

Considering the air interface between the IoT tags and the UAV flying HetNode, the S-curve parameters for the urban and rural environments are set as $a = 11.95, \sigma = 0.14$, also the coefficients of path loss are considered to be $\mu_1 = 3\ dB, \mu_2 = 23\ dB$ for LOS and NLOS respectively [33]. The path loss exponent is assumed as $\delta = 2$. Other simulation parameters are stated in Table 1.

In simulation, the three riding modes are configured as follows:

- In mode 1 multiple IoT tags can ride the signal of the Primary User (PU) and utilize the whole resource blocks allocated for that PU, in the simulation setup this mode is configured with IoT tags' ridden signal bandwidth equals to 180 kHz. Besides, all IoT tags shared the riding of the same PU downlink signal configured as interfering entities.
- In the simulation setup, mode 2 is configured where each IoT tag can ride only one subcarrier and utilize a bandwidth of 15 kHz. Besides, 12 IoT tags can utilize the whole resource block and configured as noninterfering entities.
- In the simulation setup, mode 3 is configured where multiple IoT tags can ride the same subcarrier's signal. So, all IoT tags shared the riding of the same subcarrier are configured as interfering entities. A round-robin method is configured to be used for the pairing between the IoT tags and the subcarriers. In this mechanism, each IoT tag cyclically rides the subcarrier signal of a PU to ensure

fair distribution of riding opportunities among the IoT tags which provides efficient utilization of the available resources and fair sharing of resources among multiple IoT tags.

B. SIMULATION RESULTS

In the proposed work Wi-Fi first association is considered as the default PUs association technique. In order to evaluate the performance of the different proposed riding modes the results were compared to the algorithm-free backscattering.

In Fig. 2 the result presents the average IoT tags data rates at different numbers of IoT tags considering the three proposed modes at 20 PUs. As shown in the figure the average achieved data rate decreases as the number of IoT tags increased in mode 1 and mode 3 as a result of the increasing interference between the IoT tags but because in mode 2 each tag rides one PU subcarrier and there is no interference between the tags, the average data rate remains constant. In the shown figure we can see that at a small number of IoT tags, the algorithm-free riding technique achieves a better average IoT tags rate but as the number of IoT tags increases the average rate decays exponentially and has the worst performance.

By comparing the three proposed riding modes, we can conclude that at a small number of IoT tags mode 1 achieved a better average IoT tags rate because the tag rides the whole resource block whereas in each of the other two modes, IoT tag rides the bandwidth of only one subcarrier, but as the increasing of the IoT tags number, mode 2 achieved the highest average IoT tags data rate due to the absence of interference between the tags. For dense backscatter networks (massive number of IoT tags "300 IoT tags in the service zone"), mode 1 achieves an average IoT tags data rate of about 15 Kbps (which is suitable for some types of mMTC applications), mode 2 achieves on the average 115 Kbps IoT tags data rate (which is suitable for most types of mMTC and low data rate URLLC applications) and mode 3 achieves on the average 25 Kbps IoT tags data rate (which is suitable for some mMTC applications).

The overall system rate at different numbers of IoT tags is shown in Fig. 3 For 20 PUs, the figure illustrates that the second mode achieved better performance in terms of total system rate because each tag rides a different subcarrier, typically when the number of associated IoT tags reach the total number of the subcarrier for all PUs the sum rate remains constant in a specific value because no more tags can ride any PU downlink signal. Whereas in mode 1, the IoT total system rate increases as the number of IoT tags increases.

For the third mode sum rate starts typically as mode 2 but with increasing the number of tags it slightly increases because more than one tag can associate with one subcarrier causing increased interference and consequently lower data rate. Also, we can see that the algorithm-free riding technique achieves a better total system rate at a small number of IoT tags, but as the number of IoT tags increases the algorithm-free riding technique becomes the worst one.

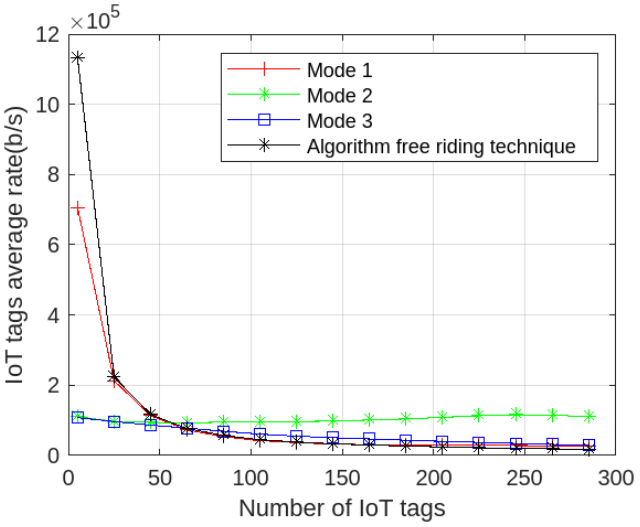

FIGURE 2. Average IoT tags data rate versus the number of IoT tags.

The degree of rate satisfaction for IoT tags (secondary system) can be measured using a sigmoid function to determine the percentage of the IoT tags that satisfy the data rate threshold R^{th}_{IoT}. In fact, this approach has been widely adopted in radio resource management and can be calculated for each IoT tag as follows.

$$\lambda_k\left(R^b_{k,m}\right) = \frac{1}{1+e^{-\beta_k\left(R^b_{k,m}-R^{th}_{IoT}\right)}}$$

where R^{th}_{IoT} is the application threshold data rate, both $R^b_{k,m}$ and R^{th}_{IoT} has the units of (b/s). β_k is a constant deciding the steepness of the satisfactory curve. It is clear from the above equation that $\lambda_k\left(R^b_{k,m}\right)$ is a monotonic increasing function with respect to $R^b_{k,m}$, i.e., individual IoT tags will feel more satisfied when they have a higher rate .λ_k of each IoT tag i is scaled between 0 and 1, i.e., $\lambda_k\left(R^b_{k,m}\right) \in (0, 1)$ and $\beta_k = 10$ [46].

Fig. 4 demonstrates the IoT tag data satisfaction rate versus the different number of tags for 20 PUs, and the rate threshold $R^{th}_{IoT} = 10\ Kbps$. It can be clearly observed from Fig. 4 that the tag data satisfaction rate decreases monotonically with an increased number of tags in mode 1 and mode 3 because when the number of IoT tags increases the IoT tags achieved data rate is decreased according to the amount of interference, in mode 3 the satisfaction ratio decreased slower than mode 1 as a result to the lower interference, while mode 2 remains constant equals to the value 1 whatever the number of IoT tags, this is because there is no interference between the tags and all tags rate requirement are satisfied. Also, we can find that the algorithm-free riding technique has the worst satisfaction rate due to that the riding is done in a random fashion without taking into consideration minimizing the interference or maximizing the IoT tags received power.

TABLE 2. IoT tags backscatter system capacity versus the number of satisfied IoT tags.

		18 PUs		21 PUs		27 PUs		30 PUs	
		Accepted	Satisfied	Accepted	Satisfied	Accepted	Satisfied	Accepted	Satisfied
Mode1	No. of IoT tags	1494	399	2875	720	2945	823	3022	1093
	Percentage of satisfied IoT tags	27%		25%		28%		36.2%	
Mode2	No. of IoT tags	216	216	252	252	324	324	360	360
	Percentage of satisfied IoT tags	100%		100%		100%		100%	
Mode3	No. of IoT tags	4484	1333	5474	1287	5608	1524	5702	1511
	Percentage of satisfied IoT tags	29.7%		23.5%		27%		26.5%	
Algorithm-free riding technique	No. of IoT tags	6000	247	6000	399	6000	428	6000	617
	Percentage of satisfied IoT tags	4.1%		6.7%		7.1%		10.3%	

TABLE 3. Interference effect on the primary system.

	Average interference power to the PUs (watt)				
No. of IoT tags	5	85	145	225	325
Mode 1	$5.79*10^{-24}$	$9.9*10^{-23}$	$1.7*10^{-22}$	$2.8*10^{-22}$	$4.5*10^{-22}$
Mode 2	$4.8*10^{-25}$	$8.3*10^{-24}$	$1.4*10^{-23}$	$2.1*10^{-23}$	$3.1*10^{-23}$
Mode 3	$4.59*10^{-25}$	$8.79*10^{-24}$	$1.6*10^{-23}$	$3.5*10^{-23}$	$4.77*10^{-23}$
Algorithm-free riding technique	$4.5*10^{-16}$	$3.8*10^{-13}$	$4.25*10^{-12}$	$2.1*10^{-9}$	$1*10^{-7}$

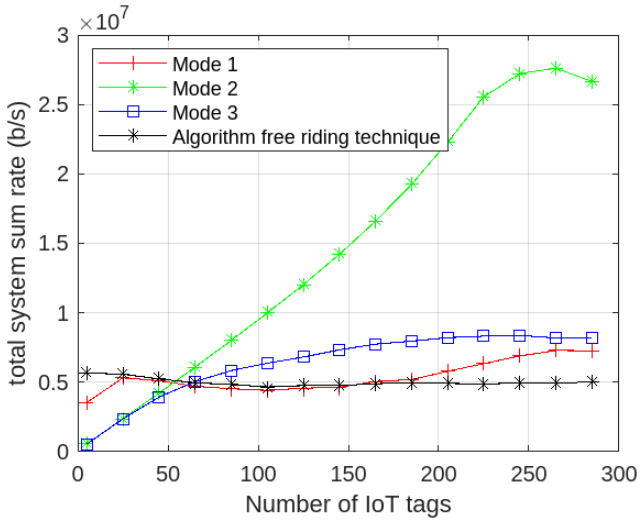

FIGURE 3. Total System rate versus the number of IoT tags.

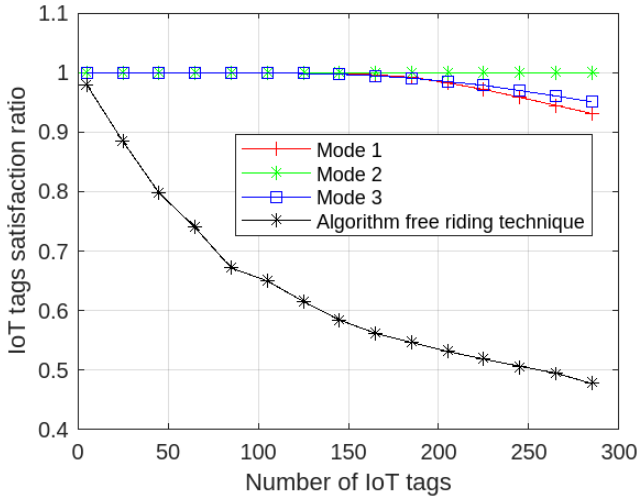

FIGURE 4. IoT tags satisfaction rate versus number of IoT tags.

In Fig. 5 we illustrate the capacity of the IoT backscatter system at different numbers of PUs, where there are 6000 IoT tags distributed uniformly within the service zone. As shown in the figure the system capacity increased as the number of PUs increased, and the algorithm-free riding technique shows the largest system capacity, this was expected because there are no stopping criteria for accepting the IoT tags association. Mode 2 shows the lowest capacity because its capacity is limited to 12 times the number of PUs, and mode 3 shows better performance than mode 1 because in mode 3 IoT tags can share riding one subcarrier of the PU signal. Fig. 5 shows that mode 3 outperforms mode 1 by 300% and outperforms mode 2 by 2,000%, which strongly supports the 6G massive IoT applications.

To compare the proposed riding modes in terms of the number of system's satisfied users that achieved the required rates to support different IoT applications (mMTC and URLLC applications), 6000 IoT tags are distributed in the service area with different numbers of PUs. Table 2 shows that in general, the number of satisfied IoT tags increased when the number of PUs increased, in the algorithm-free riding technique all IoT tags will be accepted with the lowest Percentage of satisfied IoT tags. The table shows that as the number of PUs increased from 18 to 30 the number of satisfied accepted IoT tags (system capacity) increased, for mode 1 the capacity

increased by about 200%, mode 2 capacity increased by about 167%, and mode 3 capacity increased by about 127%.

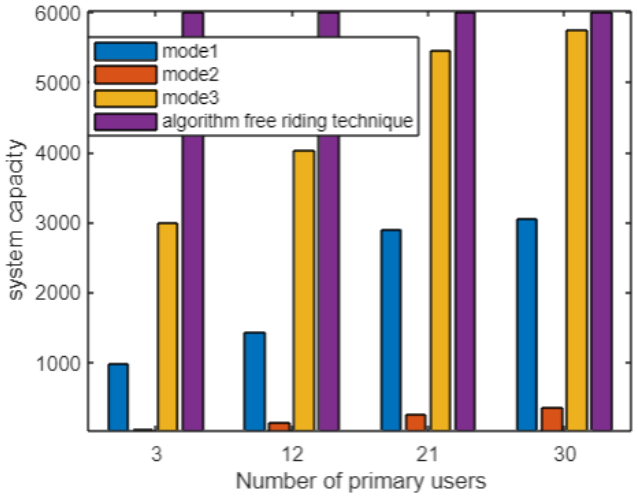

FIGURE 5. System capacity versus the number of PUs.

Also, when the number of PUs increased from 18 to 30 the number of satisfied IoT tags increased by 274% for mode 1, by 167% for mode 2, and by 113% for mode 3. On the other hand, mode 3 has the greatest capacity with the highest number of satisfied IoT tags, generally as the number of PUs increased the percentage of satisfied IoT tags increased due to the decrease of interference except for mode 2 where all accepted IoT tags have a satisfied rate. The algorithm-free riding technique accepts all IoT tags at the expense of the number of satisfied IoT, and as the number of PUs increased the percentage of accepted IoT tags increased due to decreasing the interference between IoT tags. Finally, we can conclude that mode 3 did the best performance in terms of the system capacity and the number of tags that achieved their rate requirements.

To explain the effectiveness of our proposed modes in reducing the effect of secondary system interference to the primary system which is very important to handle to keep the PUs data rate within the required range, Table 3 shows that mode 2 is the mode with the lowest interference to the PUs with the cost of achieved system capacity.

Also, Table 3 explains how the interference to the PU increased when the number of IoT tags increased and the effectiveness of our modes in reducing this interference compared to the algorithm-free riding. As seen from Table 3 when the number of IoT tags increased from 5 to 325, the PUs average interference increased by 77% in the first mode, and by 64.58% in the second mode, by 103.9% in the third mode, and by 222×10^6% in the algorithm-free riding technique. It can be seen clearly that the proposed algorithm supports the massive IoT applications over the backscatter secondary system with minimal effect on the primary system users' achieved rate and keeps the PUs data rate within the required range.

Fig. 6 shows the effect of increasing the number of PUs on the IoT total system data rate of the different proposed modes. From Fig. 6 (a) it can be noticed that for mode 1 by increasing the number of PUs from 9 to 30 the IoT total system rate increases by 24.4% at 25 IoT tags and by 39.7% at 85 IoT tags, this can be subjected to the interference decreasing between IoT tags because a smaller number of tags will associate the downlink signal dedicated to a PU. Fig. 6 (b) shows that as the number of PUs increased the IoT total system rate of mode 2 increased, this is because more IoT tags can be accepted to successfully send their data, in this mode the number of associated IoT tags is 12 times the number of PUs, from this relation the number of associated tags is increased by increasing the number of PUs.

On average, the total system rate is increased by 168.3 % by increasing the number of PUs by 2.3%. In order to show the effect of increasing the number of PUs in the third mode. Fig. 6 (c) compares the IoT total system rate at different numbers of PUs, it can be noticed that the total rate increased by 25% when the number of PUs increased from 6 to 15 at 100 IoT tags, and by 88.9% at 305 IoT tags, and by 88.9%. we can note that at 305 IoT tags when the number of PUs increased from 6 to 9 the system rate increased by 51.5%, and on the average the system rate increased by 25.9%.

In Fig. 7 (a), (b), and (c), we investigate the effect of backscatter reflection coefficient value on the IoT tags sum rate in mode 1, mode 2, and mode 3 respectively. It can be noticed that the total data rate achieved by IoT tags has better performance at larger values of backscatter coefficient α, this is because more power will be received by the UAV flying HetNode backscatter receiver because α indicates how effectively the tag reflects or scatters the incident RF signal. A higher backscatter coefficient implies that a larger portion of the incoming signal is reflected back toward the receiver, allowing for better communication reliability. Conversely, a lower RC may result in reduced communication range and reliability. Also, we can notice that the enhancement rate of the overall system rate is higher at the lower value of the backscatter reflection coefficient.

It can be noticed that for mode 1 when α increased from 0.2 to 0.5 the overall system rate enhanced by 14.5%, and when α increased from 0.8 to 1 the overall system rate enhanced by 5.6%. For mode 2 when α increased from 0.2 to 0.5 the overall system rate enhanced by 50%, and when α increased from 0.8 to 1 the overall system rate enhanced by 4.4%. For mode 3 when α increased from 0.2 to 0.5 the overall system rate enhanced by 27.1%, and when α increased from 0.8 to 1 the overall system rate enhanced by 1.3%.

It is obtained clearly that at higher values of the reflection coefficient the enhancement in the overall system rate can be neglected compared to the increased interference effect on the primary system Users.

Table 4 illustrates the effect of increasing the serving UAV Flying HetNodes on the system data rate for 15 PUs and 500 IoT tags in the service area, it can be noticed that the system rate increased when the number of UAV Flying

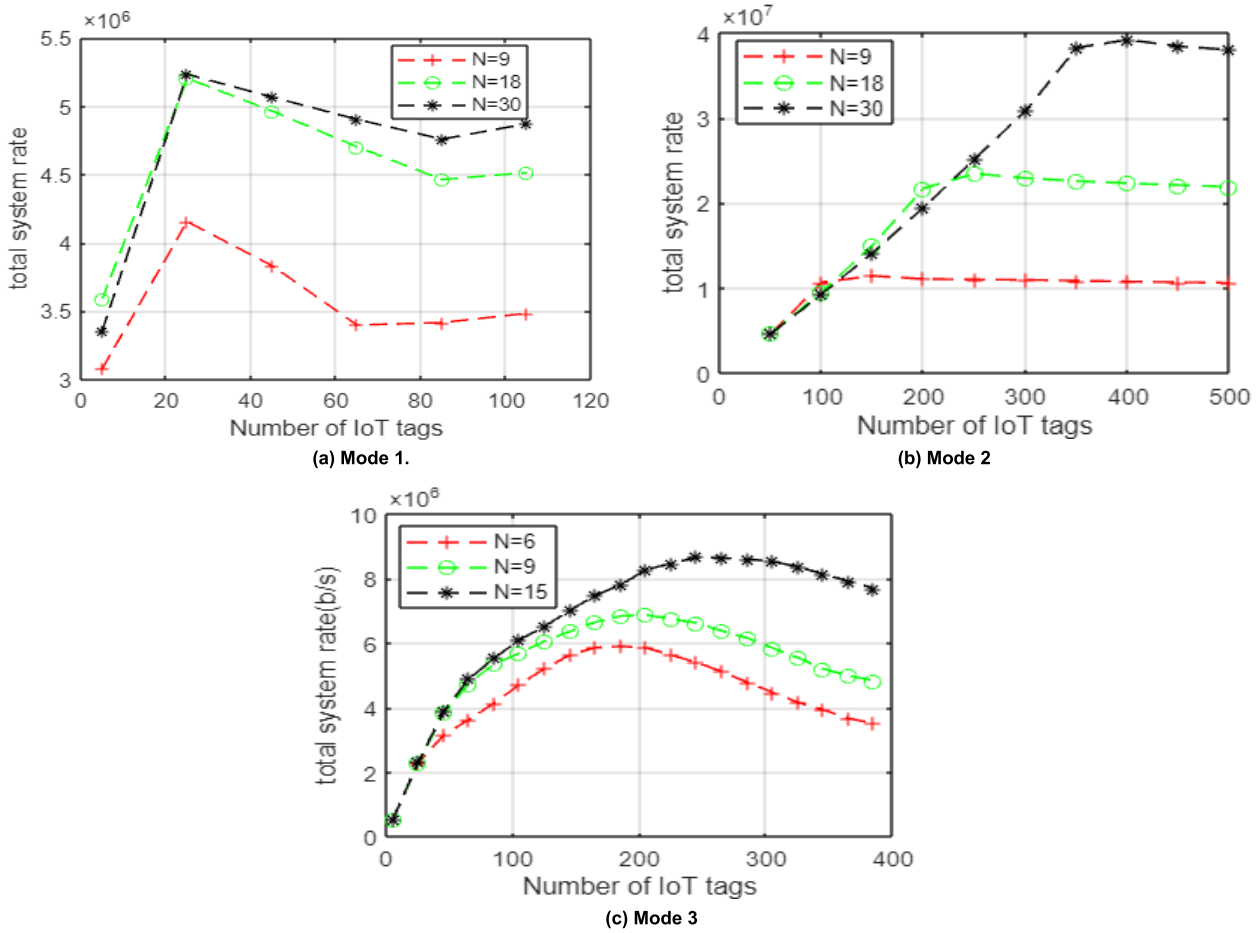

FIGURE 6. IoT total system rate at different numbers of PUs in the three proposed riding modes.

HetNodes increased because this improves the channels gain between IoT tags within the cluster and it's serving UAV flying HetNode, and reduces the interference with the other clusters.

This results in a stronger received signal strength at the receiver node and with a lower interference level, therefore the result is enhanced SINR for each tag. When the number of UAV Flying HetNodes increased from 1 to 11, the total system rate increased by 3.83% for mode 1 and increased by 11.11% for mode 2 finally the total system rate increased by 5.57% for mode 3. When the number of UAV Flying HetNodes increased from 11 to 31, the total system rate increased by 0.88% for mode 1 and increased by 2.1% for mode 2 finally the total system rate increased by 1.98% for mode 3. We can find that the IoT total system rate increased slightly with a large increase in the number of UAV Flying HetNodes, which implies that the proposed algorithm can serve a dense massive IoT service area with a small number of UAV Flying HetNodes and produce an acceptable rate performance.

C. TIME COMPLEXITY CALCULATION

From the time complexity point of view, the proposed algorithm runs in two phases, the matching game for the IoT tags association phase and the K-means++ algorithm for the IoT tags clustering phase. The time complexity of the matching game phase heavily depends on the convergence time of the matching game and is typically denoted as O(N k + N log K), where N represents the number of PUs and K denotes the number of IoT tags. On the other hand, the K-means++ clustering phase time complexity is commonly expressed as O(I K M), where I represents the number of iterations required for convergence, and M represents the number of clusters. Finally, the time complexities of the two phases are added, resulting in a comprehensive time complexity of O(NK + N log K + I K M). Whereas, the time complexity of the algorithm-free riding technique can be calculated as O(I K M). Thus, while our algorithm exhibits higher time complexity compared to the algorithm-free riding technique, it provides superior performance in terms of the system rate and the resulting interference to the primary system.

TABLE 4. IoT total system rate at different numbers of serving UAV flying HetNodes.

Serving UAV Flying HetNodes	1	11	31
Mode 1 system rate (b/s)	$1.20*10^7$	$1.246*10^7$	$1.257*10^7$
Mode 2 system rate (b/s)	$1.8*10^7$	$2*10^7$	$2.042*10^7$
Mode 3 system rate (b/s)	$7.18*10^6$	$7.58*10^6$	$7.73*10^6$

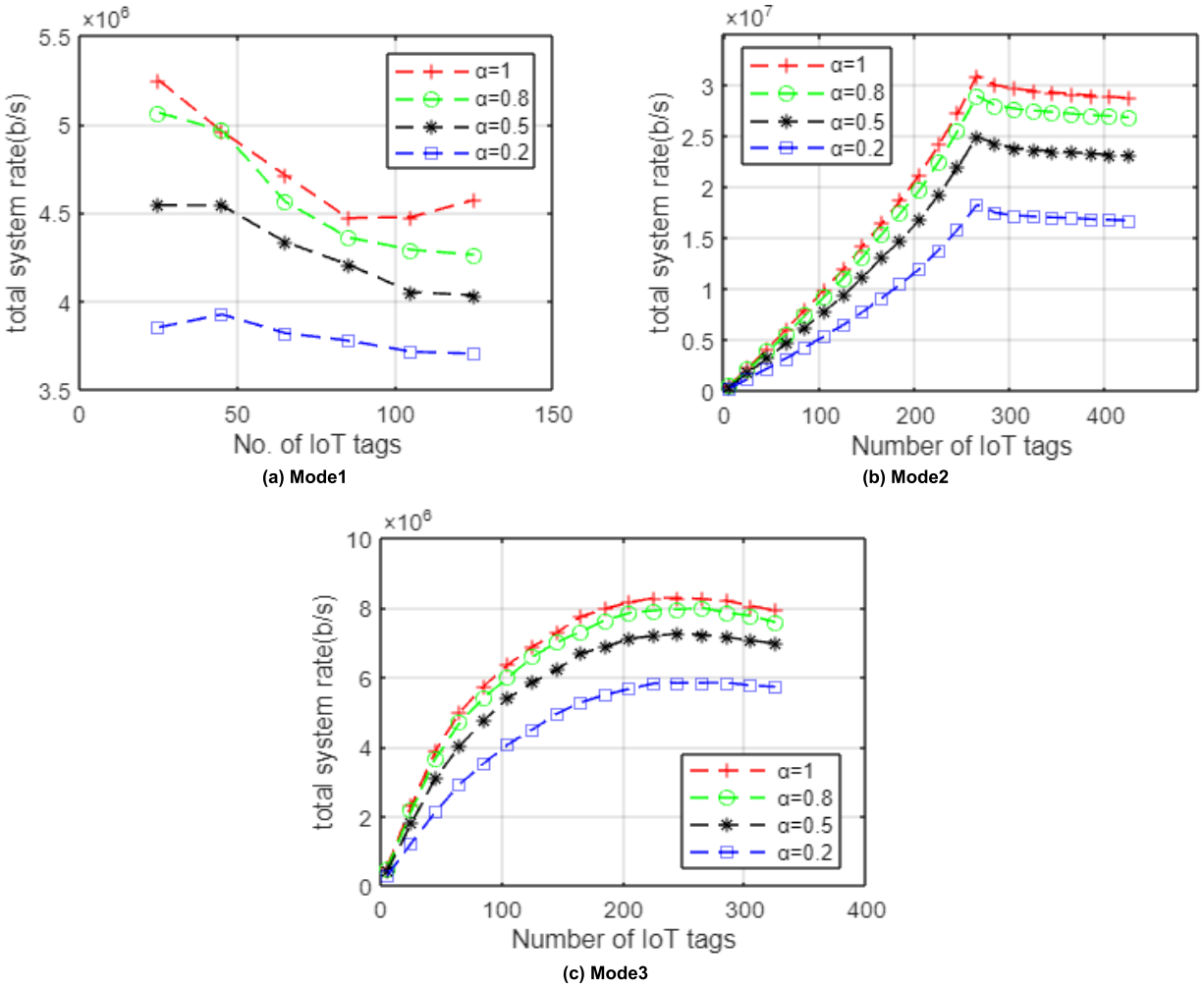

FIGURE 7. Total IoT tags system rate at different values of backscatter reflection coefficient α in the three modes.

VII. CONCLUSION

In this paper, a framework is proposed to optimize the association of IoT tags with the base station's primary users, then the associated tags ride the downlink RF signal of the selected PU, which maximizes the uplink data rate of the tags. This selection is done by taking into consideration the minimization of the resulting interference to the PU and the maximization of the IoT tags received RF signal strength from the PU's base station. The IoT tags association problem was formulated as a many-to-one matching game whereas an enhanced k-means algorithm is used for clustering IoT tags to M clusters the centroid of each cluster is considered as the optimum UAV Flying HetNode backscatter receiver location for this cluster.

Three riding modes are proposed describing how the tags ride the PU ambient signal, where the first mode is the default riding mode where all IoT tags share the riding of a specific PU downlink OFDM signal resource blocks as long as the resulting interference to this PU doesn't affect its data rate requirements. The second mode is proposed as enhanced mode, where each IoT tag rides only one subcarrier of the PU downlink OFDM signal to increase the average tags rate, also the third mode is the second enhanced mode, where each group of IoT tags can share the riding of one subcarrier of the downlink RF signal as long as the resulting average interference doesn't affect this PU's data rate requirements.

The simulation results of the proposed algorithm showed that mode 2 achieved the highest average IoT tags data rate and total system rate with the lowest interference to the PUs, over the other modes and the algorithm-free backscattering technique, where the three modes achieve average IoT tags rates in the range of 15 Kbps to 115 Kbps which can support the required rate for most mMTC and low data rate URLLC IoT applications.

On the other hand, the algorithm-free backscattering technique shows the largest system capacity with the lower percentage of satisfaction ratio (7% on the average). The capacity and satisfaction ratio of the proposed mode 3 outperforms mode 1 by 300% and 138% respectively and outperforms mode 2 by 2,000% and 420% respectively. The

proposed algorithm reduces the interference power to the PUs on the average by $1 : (15.69 \times 10^{-12})$ relative to the algorithm-free backscattering technique. Although our algorithm demonstrates a higher time complexity compared to the algorithm-free riding technique, it provides a higher performance in terms of the system rate and the resulting interference to the primary system.

Finally, we can conclude that mode 3 did the best performance in terms of the system capacity and the number of tags that achieved their rate requirements. Mode 2 achieves the best performance in terms of the average IoT tags rate and the total system rate with the highest satisfaction ratio but with the lowest achieved system capacity. It can be seen clearly that the proposed algorithm supports different IoT applications where, for massive ones mode 3 can be used, and for applications that require a high data rate mode 2 can be used. Also, the three proposed modes can support most mMTC and low data rate URLLC IoT applications and achieve the required data rates with minimal effect on the primary system users' achieved rate and keep the PUs data rate within the required range.

REFERENCES

[1] V. Liu, A. Parks, V. Talla, S. Gollakota, D. Wetherall, and J. R. Smith, "Ambient backscatter: Wireless communication out of thin air," *ACM SIGCOMM Comput. Commun. Rev.*, vol. 43, no. 4, pp. 39–50, Sep. 2013, doi: 10.1145/2534169.2486015.

[2] W. Zhao, G. Wang, R. Fan, L.-S. Fan, and S. Atapattu, "Ambient backscatter communication systems: Capacity and outage performance analysis," *IEEE Access*, vol. 6, pp. 22695–22704, 2018, doi: 10.1109/ACCESS.2018.2828021.

[3] G. Yang, Q. Zhang, and Y.-C. Liang, "Cooperative ambient backscatter communications for green Internet-of-Things," 2018, *arXiv:1801.01249*.

[4] H. Guo, Q. Zhang, S. Xiao, and Y.-C. Liang, "Exploiting multiple antennas for cognitive ambient backscatter communication," *IEEE Internet Things J.*, vol. 6, no. 1, pp. 765–775, Feb. 2019, doi: 10.1109/JIOT.2018.2856633.

[5] X. Lu, D. Niyato, H. Jiang, D. I. Kim, Y. Xiao, and Z. Han, "Ambient backscatter assisted wireless powered communications," *IEEE Wireless Commun.*, vol. 25, no. 2, pp. 170–177, Apr. 2018, doi: 10.1109/MWC.2017.1600398.

[6] D. T. Hoang, D. Niyato, P. Wang, D. I. Kim, and Z. Han, "Ambient backscatter: A new approach to improve network performance for RF-powered cognitive radio networks," *IEEE Trans. Commun.*, vol. 65, no. 9, pp. 3659–3674, Sep. 2017, doi: 10.1109/TCOMM.2017.2710338.

[7] R. Kishore, S. Gurugopinath, P. C. Sofotasios, S. Muhaidat, and N. Al-Dhahir, "Opportunistic ambient backscatter communication in RF-powered cognitive radio networks," *IEEE Trans. Cognit. Commun. Netw.*, vol. 5, no. 2, pp. 413–426, Jun. 2019, doi: 10.1109/TCCN.2019.2907090.

[8] G. Yang, D. Yuan, Y.-C. Liang, R. Zhang, and V. C. M. Leung, "Optimal resource allocation in full-duplex ambient backscatter communication networks for wireless-powered IoT," *IEEE Internet Things J.*, vol. 6, no. 2, pp. 2612–2625, Apr. 2019.

[9] A. E. Mostafa and V. W. S. Wong, "Transmit or backscatter: Communication mode selection for narrowband IoT systems," *IEEE Trans. Veh. Technol.*, vol. 71, no. 5, pp. 5477–5491, May 2022.

[10] M. Chen, Y. Miao, Y. Hao, and K. Hwang, "Narrow band Internet of Things," *IEEE Access*, vol. 5, pp. 20557–20577, 2017.

[11] *Copyright 2017 5G Americas—5G Services and Use Cases November 2017*, 5G Americas, Bellevue, WA, USA, White Paper, 2017, pp. 1–52.

[12] C. Bockelmann, N. Pratas, H. Nikopour, K. Au, T. Svensson, C. Stefanovic, P. Popovski, and A. Dekorsy, "Massive machine-type communications in 5G: Physical and MAC-layer solutions," *IEEE Commun. Mag.*, vol. 54, no. 9, pp. 59–65, Sep. 2016, doi: 10.1109/MCOM.2016.7565189.

[13] R. Kumar, D. Sinwar, and V. Singh, "QoS aware resource allocation for coexistence mechanisms between eMBB and URLLC: Issues, challenges, and future directions in 5G," *Comput. Commun.*, vol. 213, pp. 208–235, Jan. 2024, doi: 10.1016/j.comcom.2023.10.024.

[14] A. Khan, A. I. Umar, S. H. Shirazi, W. Ishaq, M. Shah, M. Assam, and A. Mohamed, "QoS-aware cost minimization strategy for AMI applications in smart grid using cloud computing," *Sensors*, vol. 22, no. 13, p. 4969, Jun. 2022, doi: 10.3390/s22134969.

[15] M. A. ElMossallamy, Z. Han, M. Pan, R. Jäntti, K. G. Seddik, and G. Y. Li, "Backscatter communications over ambient OFDM signals using null subcarriers," in *Proc. IEEE Global Commun. Conf. (GLOBECOM)*, Dec. 2018, pp. 1–6, doi: 10.1109/GLOCOM.2018.8647245.

[16] K. Ruttik, X. Wang, J. Liao, R. Jäntti, and P.-H. Dinh-Thuy, "Ambient backscatter communications using LTE cell specific reference signals," in *Proc. IEEE 12th Int. Conf. RFID Technol. Appl. (RFID-TA)*, Sep. 2022, pp. 67–70, doi: 10.1109/RFID-TA54958.2022.9923964.

[17] B. Ji, B. Xing, K. Song, C. Li, H. Wen, and L. Yang, "The efficient BackFi transmission design in ambient backscatter communication systems for IoT," *IEEE Access*, vol. 7, pp. 31397–31408, 2019, doi: 10.1109/ACCESS.2019.2899001.

[18] T. Nguyen, Y. Shin, J. Kim, and D. Kim, "Signal detection for ambient backscatter communication with OFDM carriers," *Sensors*, vol. 19, no. 3, p. 517, Jan. 2019, doi: 10.3390/s19030517.

[19] G. Yang, Y.-C. Liang, R. Zhang, and Y. Pei, "Modulation in the air: Backscatter communication over ambient OFDM carrier," 2017, *arXiv:1704.02245*.

[20] D. Bharadia, K. R. Joshi, M. Kotaru, and S. Katti, "BackFi: High throughput Wi-Fi backscatter," *ACM SIGCOMM Comput. Commun. Rev.*, vol. 45, pp. 283–296, Aug. 2015, doi: 10.1145/2785956.2787490.

[21] G. Yang and Y.-C. Liang, "Backscatter communications over ambient OFDM signals: Transceiver design and performance analysis," in *Proc. IEEE Global Commun. Conf. (GLOBECOM)*, Dec. 2016, pp. 1–6, doi: 10.1109/GLOCOM.2016.7841620.

[22] X. Wu, X. Jiang, B. Li, N. Zhao, P. Li, Y. Li, and A. Nallanathan, "Rate maximization of UAV-assisted ambient backscatter communications," *IEEE Wireless Commun. Lett.*, vol. 13, no. 3, pp. 706–710, Mar. 2024, doi: 10.1109/LWC.2023.3340242.

[23] G. M. Salama, S. S. Metwly, E. G. Shehata, and A. M. A. El-Haleem, "Deep reinforcement learning based algorithm for symbiotic radio IoT throughput optimization in 6G network," *IEEE Access*, vol. 11, pp. 42331–42342, 2023, doi: 10.1109/ACCESS.2023.3271423.

[24] M. Jiang, K.-W. Chin, and S. Soh, "Maximizing flow rates in multihop two-tier IoT networks with ambient backscattering tags," *IEEE Internet Things J.*, vol. 9, no. 24, pp. 24628–24642, Dec. 2022, doi: 10.1109/JIOT.2022.3192905.

[25] T. Hara, R. Takahashi, and K. Ishibashi, "Ambient OFDM pilot-aided backscatter communications: Concept and design," *IEEE Access*, vol. 9, pp. 89210–89221, 2021, doi: 10.1109/ACCESS.2021.3091183.

[26] A. Y. Zakariya, S. I. Rabia, and W. K. Zahra, "Optimal decision making in multi-channel RF-powered cognitive radio networks with ambient backscatter capability," *Comput. Netw.*, vol. 189, Apr. 2021, Art. no. 107907, doi: 10.1016/j.comnet.2021.107907.

[27] L. Zhang, G. Feng, S. Qin, Y. Sun, and B. Cao, "Access control for ambient backscatter enhanced wireless Internet of Things," *IEEE Trans. Wireless Commun.*, vol. 21, no. 7, pp. 5614–5628, Jul. 2022, doi: 10.1109/TWC.2022.3142327.

[28] Z. Chi, X. Liu, W. Wang, Y. Yao, and T. Zhu, "Leveraging ambient LTE traffic for ubiquitous passive communication," in *Proc. Annu. Conf. ACM Special Interest Group Data Commun. Appl., Technol., Archit., Protocols Comput. Commun.*, Jul. 2020, pp. 172–185, doi: 10.1145/3387514.3405861.

[29] D. Li and Y.-C. Liang, "Adaptive ambient backscatter communication systems with MRC," *IEEE Trans. Veh. Technol.*, vol. 67, no. 12, pp. 12352–12357, Dec. 2018, doi: 10.1109/TVT.2018.2871154.

[30] S. Idrees, X. Zhou, S. Durrani, and D. Niyato, "A retrodirective wireless power transfer scheme for ambient backscatter systems," in *Proc. IEEE Int. Conf. Commun. (ICC)*, Jun. 2020, pp. 1–6, doi: 10.1109/ICC40277.2020.9148677.

[31] T. O. Timoudas, R. Du, and C. Fischione, "Enabling massive IoT in ambient backscatter communication systems," in *Proc. ICC - IEEE Int. Conf. Commun. (ICC)*, Dublin, Ireland, Jun. 2020, pp. 1–6, doi: 10.1109/ICC40277.2020.9149022.

[32] M. Nemati, M. Soltani, J. Ding, and J. Choi, "Subcarrier-wise backscatter communications over ambient OFDM for low power IoT," *IEEE Trans. Veh. Technol.*, vol. 69, no. 11, pp. 13229–13242, Nov. 2020, doi: 10.1109/TVT.2020.3022352.
[33] X. Liu, Y. Liu, and Y. Chen, "Reinforcement learning in multiple-UAV networks: Deployment and movement design," *IEEE Trans. Veh. Technol.*, vol. 68, no. 8, pp. 8036–8049, Aug. 2019, doi: 10.1109/TVT.2019.2922849.
[34] Y. Sun, T. Wang, and S. Wang, "Location optimization and user association for unmanned aerial vehicles assisted mobile networks," *IEEE Trans. Veh. Technol.*, vol. 68, no. 10, pp. 10056–10065, Oct. 2019, doi: 10.1109/TVT.2019.2933560.
[35] S. Lhazmir, O. A. Oualhaj, A. Kobbane, and J. Ben-Othman, "Matching game with no-regret learning for IoT energy-efficient associations with UAV," *IEEE Trans. Green Commun. Netw.*, vol. 4, no. 4, pp. 973–981, Dec. 2020, doi: 10.1109/TGCN.2020.3008992.
[36] N. Van Huynh, D. Thai Hoang, X. Lu, D. Niyato, P. Wang, and D. In Kim, "Ambient backscatter communications: A contemporary survey," 2017, *arXiv:1712.04804*.
[37] C. Xu, L. Yang, and P. Zhang, "Practical backscatter communication systems for battery-free Internet of Things: A tutorial and survey of recent research," *IEEE Signal Process. Mag.*, vol. 35, no. 5, pp. 16–27, Sep. 2018, doi: 10.1109/MSP.2018.2848361.
[38] M. Anany, M. M. Elmesalawy, and A. M. A. El-Haleem, "Matching game-based cell association in multi-RAT HetNet considering device requirements," *IEEE Internet Things J.*, vol. 6, no. 6, pp. 9774–9782, Dec. 2019, doi: 10.1109/JIOT.2019.2931448.
[39] H. Hassan, I. Ahmed, R. Ahmad, H. Khammari, G. Bhatti, W. Ahmed, and M. M. Alam, "A machine learning approach to achieving energy efficiency in relay-assisted LTE—A downlink system," *Sensors*, vol. 19, no. 16, p. 3461, Aug. 2019, doi: 10.3390/s19163461.
[40] J. Cui, Z. Ding, P. Fan, and N. Al-Dhahir, "Unsupervised machine learning-based user clustering in millimeter-wave-NOMA systems," *IEEE Trans. Wireless Commun.*, vol. 17, no. 11, pp. 7425–7440, Nov. 2018, doi: 10.1109/TWC.2018.2867180.
[41] P. Fränti and S. Sieranoja, "How much can k-means be improved by using better initialization and repeats?" *Pattern Recognit.*, vol. 93, pp. 95–112, Sep. 2019, doi: 10.1016/j.patcog.2019.04.014.
[42] Q. N. Le, V.-D. Nguyen, O. A. Dobre, N.-P. Nguyen, R. Zhao, and S. Chatzinotas, "Learning-assisted user clustering in cell-free massive MIMO-NOMA networks," *IEEE Trans. Veh. Technol.*, vol. 70, no. 12, pp. 12872–12887, Dec. 2021, doi: 10.1109/TVT.2021.3121217.
[43] I. Santos, P. Vieira, R. Borralho, M. P. Queluz, and A. Rodrigues, "Emulating a software defined LTE radio access network towards 5G," in *Proc. Int. Conf. Commun. (COMM)*, Jun. 2018, pp. 1–376, doi: 10.1109/ICComm.2018.8484764.
[44] J. Qian, A. N. Parks, J. R. Smith, F. Gao, and S. Jin, "IoT communications with M-PSK modulated ambient backscatter: Algorithm, analysis, and implementation," *IEEE Internet Things J.*, vol. 6, no. 1, pp. 844–855, Feb. 2019, doi: 10.1109/JIOT.2018.2861401.
[45] A. Daeinabi, K. Sandrasegaran, and X. Zhu, "Performance evaluation of cell selection techniques for picocells in LTE-advanced networks," in *Proc. 10th Int. Conf. Electr. Eng./Electron., Comput., Telecommun. Inf. Technol.*, May 2013, pp. 1–6.
[46] M. Sheng, C. Xu, X. Wang, Y. Zhang, W. Han, and J. Li, "Utility-based resource allocation for multi-channel decentralized networks," *IEEE Trans. Commun.*, vol. 62, no. 10, pp. 3610–3620, Oct. 2014, doi: 10.1109/TCOMM.2014.2357028.

AMANY A. KHALIFA received the B.Sc. degree in electronics and communications engineering from Al-Azhar University, Cairo, Egypt, in 2015. She is currently pursuing the M.Sc. degree in electronics and communication engineering. Since 2020, she has been a Teaching Assistant with the Electronics and Communication Department, Faculty of Engineering, Egyptian Russian University. Her current research interests include mobile communication, the Internet of Things (IoT), AI applications in wireless communication, LTE–WLAN communication, unmanned aerial vehicle (UAV) communications, 6G technologies, backscatter communication, and 5G and 6G radio access networks.

AHMED M. ABD EL-HALEEM (Member, IEEE) received the B.Sc., M.Sc., and Ph.D. degrees in electronics and communications engineering from Helwan University, Cairo, Egypt, in 2001, 2006, and 2012, respectively. He is currently an Associate Professor with the Electronics and Communications Engineering Department, Faculty of Engineering, Helwan University. He is a Co-PI/Member of several research projects funded by national and international funding agencies, such as National Telecommunication Regulatory Authority (NTRA)—Egypt and Erasmus+. His current research interests include mobile/vehicular ad-hoc communication networks, 5G and 6G radio access networks, cognitive radio networking, device-to-device communication, the Internet of Things (IoT), reconfigurable intelligent surface (RIS), AI applications in wireless communication, and smart grid communication systems.

MAHMOUD M. ELMESALAWY (Member, IEEE) was born in Cairo, Egypt, in 1981. He received the B.S., M.S., and Ph.D. degrees in electronics and communications engineering from Helwan University, Cairo, in 2002, 2005, and 2010, respectively. He is currently an Associate Professor with the Department of Electronics and Communications, Engineering, Helwan University, where he is also the Director of the Wireless Research Laboratory (WRL). He is a PI/Co-PI of several research projects funded by national and international sponsors, such as the National Telecommunication Regulatory Authority (NTRA)—Egypt and Erasmus+. His current research interests include cloud radio access networks, heterogeneous cellular networks, device-to-device communications, the Internet of Things, mobile data offloading, and smart grid communication systems.

HESHAM M. Z. BADR received the B.Sc. and M.Sc. degrees in electrical engineering from Assiut University, Assiut, Egypt, in 1993 and 1999, respectively, and the Ph.D. degree in electrical engineering from Louisiana State University (LSU), Baton Rouge, LA, USA, in 2006. Since 2006, he joined the Faculty of Engineering, Helwan University, Cairo, Egypt, where he is currently an Assistant Professor with the Electronics and Communications Engineering Department. From 1994 to 1999, he was a Teaching Assistant with the Department of Electrical Engineering, Assiut University, Assiut, Egypt. From 2001 to 2006, he was an Assistant Lecturer with the Department of Electrical and Computer Engineering, LSU. His current research interests include statistical signal processing, cognitive radio networking, device-to-device communication, and AI applications in wireless communication.